APPROXIMATE ANALYSIS OF HEAT TRANSFER IN TRANSPIRED BOUNDARY LAYERS WITH EFFECTS OF PRANDTL NUMBER

TSE-FOU ZIEN*

Naval Ordnance Laboratory, Silver Spring, MD 20910, U.S.A.†

Abstract—A simple procedure is developed for approximate calculations of wall heat-transfer rates in transpired boundary layers. Applications of this procedure are illustrated by various examples of incompressible, laminar flows in the limits of large and small Prandtl numbers. A distinguished limit of large Prandtl number and small mass-transfer rate is easily identified, and some limiting solutions are presented for the porous-plate configuration. Calculations for the cases with small Prandtl numbers explicitly demonstrate the usefulness of the method in studying transient heat-conduction problems. The remarkable combination of accuracy and simplicity represents the principal merit of the method.

NOMENCLATURE

a, radius of a circular cylinder;

C_f, skin-friction coefficient, $\tau_w/\frac{1}{2}\rho u_\infty^2$;

C_p, specific heat of gas at constant pressure;

erfc, complementary error function;

F, $\frac{1}{2}C_f$;

g, profile for dimensionless temperature, $\dfrac{T-T_\infty}{T_w - T_\infty}$;

$g_1(\eta)$, $1-\eta$;

$g_4(\eta)$, $1-2\eta+2\eta^3-\eta^4$;

K–P, Karman–Pohlhausen;

k, heat conductivity of the gas;

N_x, Nusselt number, $\dot{q}_w x/(T_w - T_\infty)k$;

N_D, Nusselt number, $2a\dot{q}_w/(T_w - T_\infty)k$;

Pr, Prandtl number, $\mu C_p/k$;

$\dot{q}$, heat flux in the direction of y;

R_D, Reynolds number based on the diameter, $2u_\infty a/v$;

R_x, Reynolds number based on x, $u_\infty x/v$;

R_δ, Reynolds number based on δ, $u_\infty \delta/v$;

R_T, Reynolds number based on δ_T, $u_\infty \delta_T/v$;

T, absolute temperature;

(u, v), velocity components corresponding to (x, y);

$(u^*, v^*),(u/u_\infty, v/u_\infty)$;

(x, y), orthogonal coordinate system with origin at the leading edge or forward stagnation point, x along the surface.

Greek symbols

(α, β, γ), velocity profile-parameters defined in [1];

$\tilde{\alpha}$, a temperature profile-parameter,
$$\int_0^1 \eta_T g(\eta_T)\,d\eta_T + \tfrac{1}{2}\int_0^1 \eta_T^2 g(\eta_T)\,d\eta_T$$
$$-\int_0^1 d\eta_T \int_0^{\eta_T} \eta_T g(\eta_T)\,d\eta_T;$$

α_1, a temperature profile-parameter,
$$\int_0^1 g(\eta_T)\,d\eta_T - \int_0^1 d\eta_T \int_0^{\eta_T} g(\eta_T)\,d\eta_T$$
$$+\int_0^1 \eta_T g(\eta_T)\,d\eta_T;$$

β, a temperature profile-parameter,
$$\int_0^1 g(\eta_T)\,d\eta_T;$$

$\tilde{\gamma}$, a temperature profile-parameter,
$$\int_0^1 \eta_T g(\eta_T)\,d\eta_T;$$

δ, thickness of velocity boundary layer;

δ_T, thickness of thermal boundary layer;

ε, basic mass-transfer parameter, v_w/u_∞;

η_T, similarity variable, y/δ_T;

θ, dimensionless temperature, $\dfrac{T-T_\infty}{T_w - T_\infty}$;

κ, thermal diffusivity, $k/(\rho C_p)$;

Λ, $\tilde{\lambda}Pr^{-2/3}$;

Λ_1, $Pr\lambda_1$;

λ, $\varepsilon x/\delta$;

$\tilde{\lambda}$, $\varepsilon R_x^{1/2}$;

λ_1, εR_T;

μ, dynamic viscosity;

v, kinematic viscosity;

ρ, density;

τ, shear stress;

ϕ, angle measured from forward stagnation point.

Subscripts

∞, condition far upstream;

e, edge of boundary layer;

w, wall condition;

0, initial condition.

*Chief, Fluid Mechanics Group, Applied Aerodynamics Division.

†Presently, Naval Surface Weapons Center, White Oak, Silver Spring, MD 20910, U.S.A.

1. INTRODUCTION

A simple, approximate method for calculating the skin friction on porous surfaces has recently been described by Zien [1, 2]. It is based on an idea, due originally to Volkov, [3], for refining the classical Karman-Pohlhausen (K–P) momentum integral technique in the boundary-layer theory, and is basically a one-parameter type of integral approach.

The chief merits of this analytical method, as illustrated in [1, 2], lie in the remarkable combination of simplicity and accuracy. The relative insensitivity of the results to the choice of velocity profiles is particularly noteworthy. These encouraging findings are indicative of the potential of the method for development into a useful tool for practical calculations of boundary-layer flows of a more complex nature. Further exploitation and extension of this new method appear warranted.

The present paper contains the development of a procedure for approximate calculations of wall heat-transfer in a transpired boundary layer. The procedure is based on a further modification and extension of Volkov's [3] original idea. Thus, the heat transfer on an aerodynamic surface is calculated by considering the energy balance across the entire, attendant (thermal) boundary layer at a local flow station. A second integration of the energy equation in the direction normal to the surface is then performed to provide an ordinary differential equation for the determination of the basic profile-parameter. To be sure, the idea of using a double-integration scheme had appeared earlier in Whitehead's [4] investigation of momentum boundary layers. However, the determination of skin friction in [4] was based on the local slope of the assumed velocity profile, as in the original K–P procedure.

For easy demonstration of the method, only simple, yet basic, flows are considered in this paper. Thus, applications are made to two-dimensional, incompressible, laminar boundary layers of a single-component fluid. Results are presented here only for limiting cases of large or small Prandtl numbers where certain simplifying approximations can be effectively exploited to further facilitate the exhibition of the central ideas of the method. Detailed results for $Pr = O(1)$ pertaining to the semi-infinite flat plate with uniform surface mass flux are available in Zien [5]. The frictional heating is neglected in the energy equation throughout the calculations, and this approximation is generally valid for incompressible boundary layers where the Eckert number is usually small. An exact and comprehensive analysis of heat transfer in a class of self-similar transpired boundary layers, including the effects of frictional heating, can be found in Gersten and Körner [6].

The method is first applied to the case of transpired boundary layers with large Prandtl numbers. A distinguished limit of large Prandtl number and small mass-transfer rate is readily apparent in the present integral formulation. Some examples of this limiting flow are studied. The procedure is then used to study a class of low Prandtl number heat-transfer problems, and the usefulness of the present method in providing approximate solutions to general transient heat-conduction problems becomes evident in the process.

It is noted here that all the calculations presented in this paper involve, at most, the numerical integration of a single, first-order ordinary differential equation. In many cases solutions are obtained in explicit, analytical forms. The primary purpose of the paper is not to present solutions to any new problems. Rather, it is to show how simply some old solutions can be reproduced with good accuracy by the present method.

2. GENERAL FORMULATION

2.1. Equations and boundary conditions

In terms of the nondimensional velocity (u^*, v^*) and temperature, θ, the basic differential equations and boundary conditions for an incompressible, constant-property, laminar boundary layer over an isothermal porous surface are:

$$\frac{\partial u^*}{\partial x} + \frac{\partial v^*}{\partial y} = 0, \tag{1a}$$

$$u^* \frac{\partial u^*}{\partial x} + v^* \frac{\partial u^*}{\partial y} = \frac{\nu}{u_\infty} \frac{\partial^2 u^*}{\partial y^2} + u_e^* \frac{\partial u_e^*}{\partial x}, \tag{1b}$$

$$u^* \frac{\partial \theta}{\partial x} + v^* \frac{\partial \theta}{\partial y} = \frac{\nu}{u_\infty} \frac{1}{Pr} \frac{\partial^2 \theta}{\partial y^2}; \tag{1c}$$

at $y = 0$:

$$u^* = 0 \tag{2a}$$

$$\theta = 1 \tag{2b}$$

$$v^* = \varepsilon \tag{2c}$$

as $y \to \infty$:

$$u^* \to 1 \tag{2d}$$

$$\theta \to 0. \tag{2e}$$

In the usual practice of integral methods, the asymptotic conditions are specified at the edges of the boundary layer, δ and δ_T, for u^* and θ, respectively. Some initial conditions on u^* and θ are generally required at $x = 0$ to complete the formulation. These initial conditions are replaced by conditions on initial boundary-layer thicknesses, $\delta(0)$ and $\delta_T(0)$, in the present integral formulation.

The skin-friction coefficient, C_f, and the Nusselt number, N_x, are related to u^* and θ through the following expressions:

$$\tfrac{1}{2} C_f = \frac{\nu}{u_\infty} \frac{\partial u^*}{\partial y} \bigg|_w \tag{3a}$$

and

$$N_x = -x \frac{\partial \theta}{\partial y} \bigg| . \tag{3b}$$

2.2. Present method of solution

Since the momentum equation is decoupled from the energy equation, the solution of u^* can proceed independently of the temperature field. In order to present a self-consistent development of the calculation procedure, we shall make use of the approximate solutions of u^* by a similar calculation scheme as reported by Zien [1, 2] for the examples to be discussed below.

We now proceed directly to solve the energy equation. The first integration of (1c) gives

$$\frac{\partial}{\partial x}\int_0^y u^*\theta\,dy + \varepsilon(\theta-1)$$

$$-\theta\frac{\partial}{\partial x}\int_0^y u^*\,dy = \frac{\kappa}{u_\infty}\left(\frac{\partial\theta}{\partial y} - \frac{\partial\theta}{\partial y}\bigg|_w\right) \quad (4)$$

where the continuity equation has been used to eliminate v^* in favor of u^*.

Equation (4) is taken as an expression for the wall heat flux by letting the integration cover the entire thermal boundary layer. Thus, using (3b), we have

$$S_t \equiv \frac{N_x}{R_x Pr} = \frac{d}{dx}\int_0^{\delta_T} u^*\theta\,dy - \varepsilon. \quad (5)$$

Equation (5) is a nondimensional version of the energy balance across the thermal boundary layer at the station x. Therefore, the surface heat transfer is determined from an integral expression involving the assumed profiles for u^* and θ. Of course, this representation would be exactly the same as the one using the derivative of θ at the wall if the profiles used for u^* and θ were the exact solutions of the problem under consideration.

The basic parameter of the thermal boundary layer, δ_T, is to be determined by the following differential equation which results from a second integration of the original energy equation. Thus, effecting another integration of (4), we arrive at

$$\int_0^{\delta_T}dy\frac{\partial}{\partial x}\int_0^y u^*\theta\,dy + \int_0^{\delta_T}\left(\varepsilon - \frac{\partial}{\partial x}\int_0^y u^*\,dy\right)\theta\,dy$$

$$= \delta_T\frac{d}{dx}\int_0^{\delta_T}u^*\theta\,dy - \frac{\kappa}{u_\infty}. \quad (6)$$

In deriving (6) use has been made of the wall heat-flux expression, (5).

We assume the following simple form for θ:

$$\theta = g(\eta_T) = \sum_{i=0}^n k_i\eta_T^i, \quad k_i = \text{const.} \quad (7)$$

The choice of the profiles is obviously crude in the sense that they presume similarity for general flows to be considered below. However, they are to be chosen such that the essential boundary conditions, (2b) and (2e), are observed.

Equation (6) reduces to a first-order, nonlinear, ordinary differential equation for δ_T, once a form for θ, such as (7), is introduced. With δ_T solved, the Stanton number, S_t, follows readily from (5) through an algebraic process.

3. APPLICATION TO CASES OF LARGE Pr

3.1. General remarks

The existing literature on boundary-layer flows with large Prandtl numbers is voluminous. Our purpose here is merely to describe the application of the present simple method to this class of flows. Hence, only the references pertinent to the present development and results will be mentioned.

For large Prandtl numbers, the simplified representation of the velocity in the thermal boundary layer is

$$u \sim \frac{\tau_w}{\mu}y. \quad (8)$$

This approximation was introduced and discussed by Fage and Falkner [7], Lighthill [8], Morgan and Warner [9], among others, and is convenient for systematic developments. Subsequent extensions and improvements of this simplifying approximation can be found, for example, in Curle [10], and more recently, Chao [11]. This simple expression will be exploited in the present formulation. The examples to be presented here are porous-plate boundary layers for which the skin friction, τ_w, has been calculated earlier by Zien [1, 2]. A self-consistent development of the procedure is thus readily accessible. The results to be presented and discussed in the following are all based on the approximate solutions of τ_w pertaining to the linear velocity profile used in [1]. However, two temperature profiles, g_1 and g_4, are used in the calculation to test the sensitivity of results to the temperature profiles. We note here that the velocity profile-parameters take the values $(\alpha, \beta, \gamma) = (1/8, 1/2, 1/6)$ in the ensuing calculations (see [1]), and the temperature profile-parameters, $(\tilde\alpha, \tilde\beta, \tilde\gamma)$ for g_1 and g_4 are $(1/8, 1/2, 1/6)$ and $(1/28, 3/10, 1/15)$, respectively.

3.2. Porous plate: similarity case

The basic equations are (5) and (6). From (8) we have

$$u^* = \tfrac{1}{2}C_f R_T\eta_T = FR_T\eta_T \quad (9)$$

where $R_T = u_\infty\delta_T/\nu$. For this particular flow, the result of F as reported by Zien [1], i.e.

$$F = R_x^{-1/2}\left(\frac{\alpha}{2} - \beta\lambda\right)^{-1/2}\left(\frac{\gamma}{2} - \lambda\right), \quad (10a)$$

will be used. Also, λ is related to $\tilde\lambda$ through

$$\tilde\lambda = \lambda\left(\frac{\alpha}{2} - \beta\lambda\right)^{-1/2}. \quad (10b)$$

Substitution of (9) into (6) leads readily to

$$\tilde\alpha R_T\frac{d}{dR_x}(R_T^2 F) = \frac{1}{Pr} + \tilde\beta\varepsilon R_T. \quad (11)$$

For the case of similarity blowing (or suction), $\varepsilon R_T = \text{const.}$, and (11) is easily integrated to give the following solution:

$$\lambda_1^3 - \left[\frac{2}{\tilde\alpha}\tilde\beta\tilde\lambda^3\frac{\left(\frac{\alpha}{2} - \beta\lambda\right)^{1/2}}{\left(\frac{\gamma}{2} - \lambda\right)}\right]\lambda_1$$

$$-\frac{2}{\tilde\alpha}\frac{1}{Pr}\tilde\lambda^3\frac{\left(\frac{\alpha}{2} - \beta\lambda\right)^{1/2}}{\left(\frac{\gamma}{2} - \lambda\right)} = 0, \quad (12)$$

where $\lambda_1 \equiv \varepsilon R_T$.

The heat transfer is obtained from (5), once R_T is found. The result is

$$\frac{N_x}{\sqrt{(R_x)}} = Pr\left[\frac{\tilde{\gamma}}{2}\left(\frac{2}{\tilde{\alpha}}\right)^{2/3}\left(\frac{1}{Pr}\right.\right.$$

$$\left.\left. + \lambda_1\beta\right)^{2/3}\left(\frac{\alpha}{2} - \beta\lambda\right)^{-1/6}\left(\frac{\gamma}{2} - \lambda\right)^{1/3} - \tilde{\lambda}\right]. \quad (13)$$

Equations (12), (13) and (10b) constitute the solution for $N_x/R_x^{1/2}$ as functions of $\tilde{\lambda}$ and Pr.

It is interesting to note the behavior of the present approximate solutions in the limit of $Pr \to \infty$ and $\tilde{\lambda} = O(1)$ for suction and blowing separately. Following limiting solutions are easily deduced from (12) and (13):

$$\tilde{\lambda} < 0: \lambda_1 \sim -\frac{1}{\beta}\frac{1}{Pr} \quad \text{and} \quad \frac{N_x}{R_x^{1/2}} \sim |\tilde{\lambda}|Pr; \quad (14)$$

$$\tilde{\lambda} > 0: \lambda_1 \sim \tilde{\lambda}^{3/2}\left[\frac{2\beta}{\tilde{\alpha}}\frac{\left(\frac{\alpha}{2} - \beta\tilde{\lambda}\right)^{1/2}}{\frac{\gamma}{2} - \lambda}\right]^{1/2} \quad \text{and}$$

$$\frac{N_x}{R_x^{1/2}} \sim Pr\,\tilde{\lambda}\left(\frac{\tilde{\gamma}}{\tilde{\alpha}}\beta - 1\right). \quad (15)$$

For the special case of $\tilde{\lambda} = 0$, the asymptotic limits for $N_x/R_x^{1/2}$ as $Pr \to \infty$ are $0.367\,Pr^{1/3}$ and $0.338\,Pr^{1/3}$ for $\theta = g_1$ and g_4, respectively. These approximate limits are to be compared with the exact limit of $0.339\,Pr^{1/3}$ (see, for example, [12]).

As $Pr \to \infty$, the heat-transfer rate predicted here approaches the correct asymptote (see Gersten and Körner [6]) independent of profiles for the case of suction. For blowing, the present solutions show a strong profile-dependent behavior. Note that the quantity in the parenthesis of (15) is negative for both profiles considered here. The implications of the above observations are thus clear. As Pr increases, the present solutions are uniformly good for suction, but predict too rapid a decay in the heat-transfer rate for blowing, especially when $\tilde{\lambda}$ is large.

Some typical results are illustrated in Figs. 1–4 and compared with the available exact solutions due to Stewart and Prober [13] and Thompson [14] whenever appropriate.

Figure 1 shows the results for $Pr = 1$ for which an exact integral, $\theta = 1 - u^*$, holds. Exact solutions for heat transfer are thus available from the exact skin-friction results of Emmons and Leigh [15], or directly from [13], for comparison. It is remarkable that the present procedure, suitable for large Prandtl numbers, yields very accurate results of heat transfer for $Pr = 1$. Of course, the finding that the validity of a calculation procedure designed for large Prandtl numbers actually extends into regions of moderate Prandtl numbers is not totally unexpected, see [8]. We also note the insensitivity of the present results to the profiles used in the calculations.

Figures 2–4 show the heat-transfer results are functions of the Prandtl number at three values of $\tilde{\lambda}$:$0\cdot01/\sqrt{2}$, $0.1/\sqrt{2}$ and $-\sqrt{2}/10$, for which exact
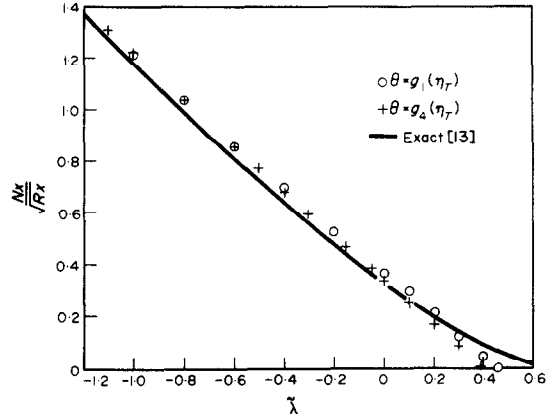

FIG. 1. Porous plate, similarity case, $Pr = 1$ (present method, $u = y\tau_w/\mu$).
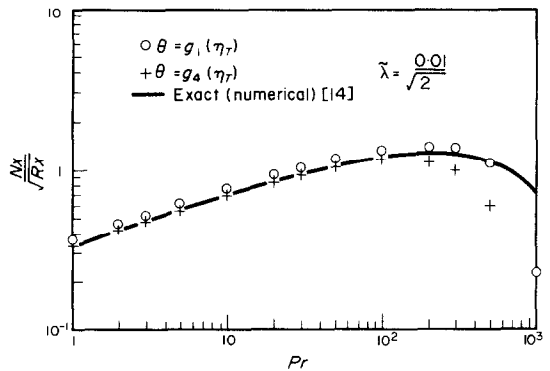

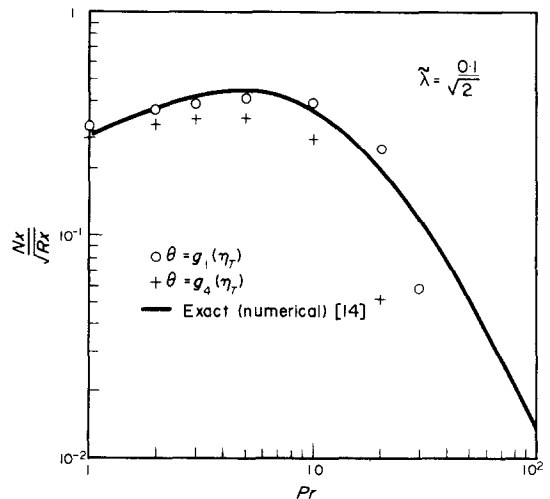FIG. 2. Porous plate, similarity blowing (present method, $u = y\tau_w/\mu$).

FIG. 3. Porous plate, similarity blowing (present method, $u = y\tau_w/\mu$).

solutions are available for comparison. These results clearly confirm our aforementioned predictions based on the behavior of the present solutions in the limit of $Pr \to \infty$. However, it should be remarked here that as $Pr \to \infty$, the results pertaining to blowing, though quantitatively inaccurate, are still qualitatively correct. It is possible that the thermal boundary layer is blown off the surface while the momentum boundary layer still remains attached.
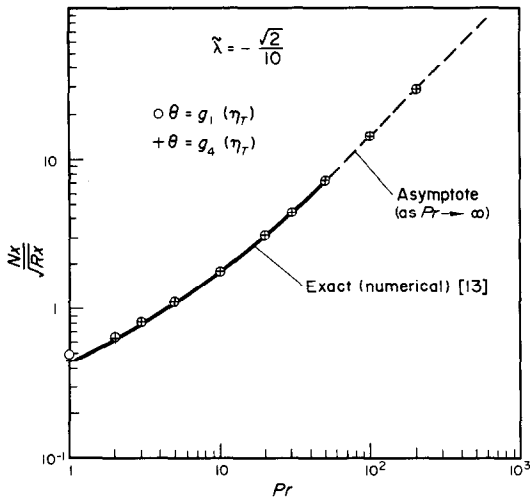
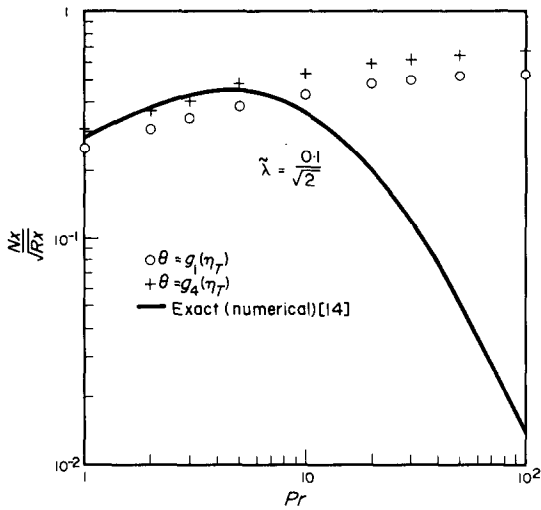FIG. 4. Porous plate, similarity suction (present method, $u = y\tau_w/\mu$).

FIG. 5. Porous plate, similarity blowing (usual K–P method, $u = y\tau_w/\mu$).

The same approach and profiles are then employed in the original K–P procedure for this problem, using τ_w obtained from the original K–P method with a linear velocity profile, as reported in [1]. The results are presented here only for $\tilde{\lambda} = 0.1/\sqrt{2}$ in Fig. 5. A comparison between Fig. 5 and Fig. 3 clearly illustrates the superiority of the refined K–P procedure. The absence of a sharp decrease of the heat-transfer rate in the interval, $6 < Pr < 100$, is typical of the failure of the original K–P procedure. Nevertheless, it should be mentioned that for the case of suction, the original K–P procedure with the same profiles is also capable of predicting the correct asymptotic behavior for $Pr \to \infty$, only the sensitivity of results to profiles is more pronounced.

3.3. A distinguished limit

The singular perturbation nature of the boundary-layer energy equation in the limit of $Pr \to \infty$ is well-known. (See, for example, Narasimha and Vasantha, [16].) It is also apparent in (1c) in which the co-

efficient of the highest derivative approaches zero as $Pr \to \infty$. The asymptotic structure of the thermal boundary layer with surface blowing in the limit of $Pr \to \infty$ has been discussed by Kassoy [17], among others. The interesting phenomenon of thermal layer blow-off is qualitatively analyzed for the case of a porous plate with similarity blowing in [17].

Physically speaking, the thermal boundary layer has a vanishing thickness relative to the momentum boundary layer as $Pr \to \infty$, because the viscous diffusion $(\sim \nu)$ dominates the thermal diffusion $(\sim \kappa)$. Therefore, the heat transfer takes place in a very thin region close to the wall where the convective velocity components (u, v) are also small. In the case of transpired boundary layers, an additional mechanism of heat transfer $(\sim \varepsilon)$ appears. The precise orders of magnitude of these physical quantities as $Pr \to \infty$ are related uniquely only in a distinguished limit in which convection, conduction and mass transfer are of equal importance. It is convenient and instructive to deduce such a limit from the equations derived in the process of the present development. We remark here that, as $Pr \to \infty$, the present method seems particularly suited for this case of vanishingly small $\tilde{\lambda}$ in view of the results discussed in Section 3.2.

Let us consider (11). The three terms from left to right represent, respectively, the effects of convection, conduction and mass transfer. Therefore, we require that, as $Pr \to \infty$,

$$\frac{R_T^3}{R_x^{3/2}} \sim \frac{1}{Pr} \sim \varepsilon R_T, \tag{16}$$

where we have used the relation $F = O(R_x^{-1/2})$.

It follows immediately that

$$Pr \to \infty : \tilde{\lambda} = O(Pr^{-2/3}), \quad \lambda_1 = O(Pr^{-1}) \quad \text{and}$$
$$\delta_T/\delta = O(Pr^{-1/3}). \tag{17}$$

Thus, the distinguished limit corresponds to vanishingly small values of $\tilde{\lambda}$ and δ_T/δ. We are now led to introduce the following variables for the study of this limiting flow:

$$\Lambda = Pr^{2/3} \tilde{\lambda} = O(1) \tag{18a}$$

$$\Lambda_1 = Pr \lambda_1 = O(1). \tag{18b}$$

In this limit, F may be expanded as

$$F = F_0 + \tilde{\lambda} F_1 + \ldots \tag{19}$$

where F_0 corresponds to the skin-friction coefficient in the absence of mass transfer. Only the leading term, F_0, will be needed in the ensuing calculations. The result to be obtained thus corresponds to an approximation of the leading asymptotic term in this distinguished limit. A systematic asymptotic analysis of the general flow in this distinguished limit appears to be an interesting problem of fundamental importance but beyond the scope of the present paper.

For a flat plate, [1] provides

$$F_0 = \frac{\gamma}{\sqrt{(2\alpha)}} R_x^{-1/2}, \tag{20}$$

and, as mentioned earlier, $(\alpha, \gamma) = (1/8, 1/6)$ is used in the calculations.
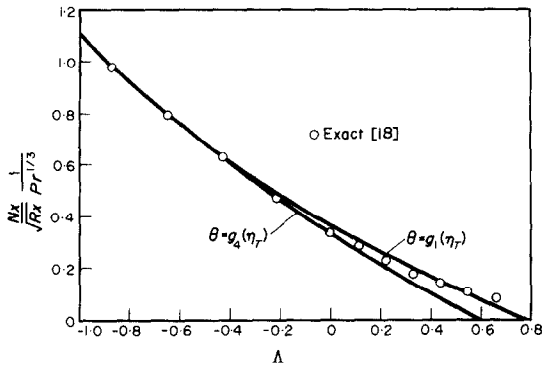
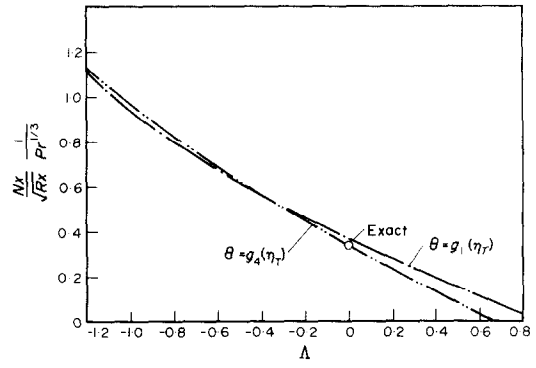FIG. 6. Porous plate, distinguished limit for similarity case (present method).

FIG. 7. Porous plate, distinguished limit for uniform ε (present method).

3.3.1. *Porous plate: similarity case.* Introducing Λ and Λ_1, and applying the limit process, (17), to (12) and (13), we arrive at the following results:

$$\Lambda_1^3 = (2)^{3/2}(\alpha)^{1/2}\Lambda^3(1+\Lambda_1\tilde{\beta})/(\tilde{\alpha}\gamma) \qquad (21)$$

and

$$\frac{N_x}{R_x^{1/2}} = Pr^{1/3}\left[\tilde{\gamma}(\alpha)^{-1/6}(\tilde{\alpha})^{-2/3}(\gamma)^{1/3}(2)^{-1/2}(1 \right. $$
$$\left. + \Lambda_1\tilde{\beta})^{2/3} - \Lambda\right]. \qquad (22)$$

Results of $N_x/(R_x^{1/2}Pr^{1/3})$ as a function of Λ for the two temperature profiles are plotted in Fig. 6. It can be shown that both curves approach the exact limit of asymptotic suction. The dependence of the results to profiles is still weak in this limiting flow, and the thermal boundary-layer blow-off ($N_x = 0$) is predicted at a finite value of Λ. An exact treatment of this limiting case was recently reported by Gersten [18] for a class of Falkner–Skan flows. The same distinguished limit was derived in a different manner in [18]. The exact solution pertaining to the flat-plate configuration is included in Fig. 6 for comparison with the present approximate results. The agreement, in general, is clearly quite satisfactory, except near thermal boundary-layer blow-off where the exact solution exhibits an exponential decay in heat transfer.

3.3.2. *Porous plate: nonsimilar case.* Equation (11) is still the basic differential equation for this nonsimilar flow, as the velocity, u, is approximated by (8). Now, applying the limit process, (17) and (18), to (11) and noting (20), we have the following differential equation for the limiting flow:

$$\frac{d\Lambda_1}{d\Lambda} = \frac{\dfrac{(8\alpha)^{1/2}}{\gamma\tilde{\alpha}}(1+\tilde{\beta}\Lambda_1)+\left(\dfrac{\Lambda_1}{\Lambda}\right)^3}{2\left(\dfrac{\Lambda_1}{\Lambda}\right)^2} \qquad (23a)$$

and

$$\Lambda \to 0, \quad \frac{\Lambda_1}{\Lambda} \to \frac{(8\alpha)^{1/6}}{(\gamma\tilde{\alpha})^{1/3}}. \qquad (23b)$$

Substituting (9) into (5) and introducing Λ and Λ_1, we obtain

$$\frac{N_x}{R_x^{1/2}} = Pr^{1/3}\left[\frac{\tilde{\gamma}}{\tilde{\alpha}}\frac{\Lambda}{\Lambda_1} - \left(1 - \frac{\tilde{\beta}\tilde{\gamma}}{\tilde{\alpha}}\right)\Lambda\right]. \qquad (24)$$

Results of $N_x/(R_x^{1/2}\,Pr^{1/3})$ as a function of Λ are plotted in Fig. 7 for the two temperature profiles used in the calculation. The behavior of heat transfer is quite analogous to that for the similarity case, Fig. 6. We also note that the two curves will converge in the region of large negative Λ and approach the exact asymptotic suction limit, $N_x/(R_x^{1/2}\,Pr^{1/3}) \sim |\Lambda|$. No other limiting solutions to this nonsimilar flow seem to exist in the literature, to the best of the author's knowledge.

4. APPLICATION TO CASES OF SMALL Pr

4.1. *General remarks*

In this section, the method is applied to the calculation of boundary-layer heat transfer in the limit of $Pr \to 0$. The mathematical limit here is $R_x \to \infty$, $Pr \to 0$ and $R_x Pr \to \infty$, so that the concept of a thin thermal layer near the surface is still valid. The chief simplification is that the velocity profile, u, inside the thermal boundary layer can be approximated by the external potential stream $u_e(x)$ [12]. Therefore, we need only to assume the temperature profile. The resulting solution corresponds to the limiting case of $Pr = 0$, i.e. an inviscid but heat-conducting fluid. Two representative examples will be presented in the following. These examples will explicitly reveal the relevance of the differential equations to a class of heat-conduction problems. Therefore, the success of the present method here would imply its potential usefulness in studying general problems in transient heat conduction with complex boundary conditions, including nonlinear cases. Some initial attempts have already been made by Volkov and Li-Orlov [19]. A more thorough investigation of this application appears desirable, and should lead to a modified version of the work of Goodman [20] who had applied the original K–P method to a variety of heat-conduction problems.

4.2. *Porous plate:* $\varepsilon = const. = O(1/\sqrt{(R_x Pr)})$

Here the velocity $(u, v) = (u_\infty, v_w)$ and the energy equation takes the form

$$\frac{\partial\theta}{\partial x} + \varepsilon\frac{\partial\theta}{\partial y} = \frac{\kappa}{u_\infty}\frac{\partial^2\theta}{\partial y^2}. \qquad (25)$$

The first and second integrations of (25) lead to, respectively,

$$\frac{N_x}{R_x Pr} = \tilde{\alpha}_1 \frac{dR_T}{dR_x} - \varepsilon \quad (26)$$

and

$$\tilde{\alpha}_1 \frac{dR_T}{dR_x} = \frac{1}{Pr R_T} + \varepsilon \tilde{\beta}. \quad (27)$$

where $(\tilde{\alpha}_1, \tilde{\beta})$ are profile-parameters defined in the Nomenclature. In deriving (26) and (27), a temperature profile of the form $\theta = g(\eta_T)$ is assumed. Equation (27) is readily integrated to give

$$\varepsilon^2 R_x Pr = \frac{\tilde{\alpha}_1}{\tilde{\beta}} \varepsilon R_T Pr - \frac{\tilde{\alpha}_1}{\tilde{\beta}^2} \ln(1 + \tilde{\beta} \varepsilon R_T Pr), \quad (28)$$

and the heat-transfer coefficient follows from (26) as

$$\frac{N_x}{\sqrt{(R_x Pr)}} = \frac{\tilde{\beta}}{\tilde{\alpha}_1} \frac{\varepsilon \sqrt{(R_x Pr)}}{\varepsilon R_T Pr} - \left(1 - \frac{\tilde{\beta}^2}{\tilde{\alpha}_1}\right) \varepsilon \sqrt{(Pr R_x)}. \quad (29)$$

Equations (28) and (29) form a parametric representation for the heat-transfer coefficient, i.e.

$$\frac{N_x}{\sqrt{(R_x Pr)}} = f\left(\varepsilon \sqrt{(R_x Pr)}\right). \quad (30)$$

Results corresponding to the two temperature profiles, g_1 and g_4, are illustrated in Fig. 8. The profile-parameters associated with g_1 and g_4 and $(\tilde{\alpha}_1, \tilde{\beta}) = (1/3, 1/2)$ and $(2/15, 3/10)$, respectively.
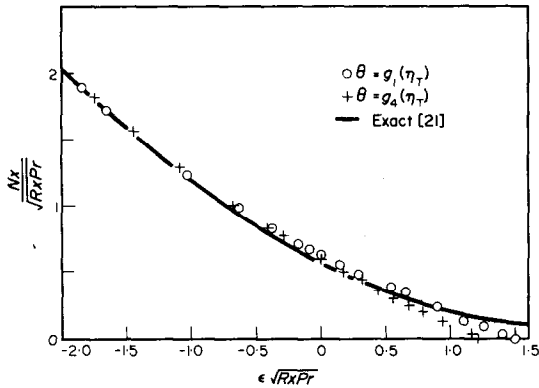
FIG. 8. Porous plate, uniform ε, $Pr \to 0$ (present method).

It is interesting to note that (25) is also relevant to the problem of the transient heat conduction in a semi-infinite solid moving with a constant velocity ε and maintained at a constant temperature at $y = 0$. The exact solution is available in Carslaw and Jaeger [21]. The heat-transfer rate is readily obtained from the solution for θ, i.e.

$$\frac{N_x}{\sqrt{(R_x Pr)}} = \frac{1}{\sqrt{\pi}} \exp\left(-\frac{\varepsilon^2 R_x Pr}{4}\right)$$
$$- \frac{\varepsilon \sqrt{(R_x Pr)}}{2} \text{erfc}\left(\frac{\varepsilon \sqrt{(R_x Pr)}}{2}\right). \quad (31)$$

The exact solution is also shown in Fig. 8 for comparison with the approximate solutions, (30). The present results are clearly very satisfactory in accuracy;

the close agreement between the results corresponding to the two temperature profiles is also evident. However, it should be pointed out that as the blowing intensity increases, the present approximate solutions predict zero heat transfer (thermal boundary-layer blow-off) at finite values of $\varepsilon \sqrt{(R_x Pr)}$, while the exact solution shows exponential decay in heat transfer. Therefore, as is usually the case, the accuracy of the present solution begins to deteriorate as the blow-off point is approached.

4.3. Circular cylinder

We now consider the case of a circular cylinder in crossflow. The orthogonal curvilinear coordinate system, (x, y), has its origin at the forward stagnation point with x measuring the distance along the surface $(x = a\phi)$. Then $u^* = 2\sin\phi$, $v^* = -2y^* \cos\phi$. The energy equation and the boundary conditions are

$$\sin\phi \frac{\partial\theta}{\partial\phi} - y^* \cos\phi \frac{\partial\theta}{\partial y^*} = \frac{1}{R_D Pr} \frac{\partial^2\theta}{\partial y^{*2}} \quad (32a)$$

$$\theta(\phi, 0) = 1 \quad \theta(\phi, \delta^*) = 0, \quad (32b)$$

where $u^* = u/u_\infty$, $v^* = v/u_\infty$, $y^* = y/a$ and $\delta^* = \delta_T/a$.

Applying the present method to (32a) results in the following two equations, based on the assumed profile, $\theta = g(\eta_T)$:

$$\frac{1}{2} \frac{N_D}{R_D Pr} = \tilde{\beta}\left(\sin\phi \frac{d\delta^*}{d\phi} + \delta^* \cos\phi\right) \quad (33)$$

and

$$\delta^* \sin\phi \frac{d\delta^*}{d\phi} + \delta^{*2} \cos\phi = \frac{1}{\tilde{\alpha}_1} \frac{1}{R_D Pr}, \quad (34a)$$

with

$$\delta^*(\phi, 0) = (\tilde{\alpha}_1 R_D Pr)^{-1/2} \equiv (\delta^*)_0. \quad (34b)$$

Equation (34a) can be easily integrated to give

$$\delta^* = (\delta^*)_0 \sec\frac{\phi}{2}. \quad (35)$$

Equation (33) then gives

$$\frac{N_D}{\sqrt{(R_D Pr)}} = 2\frac{\tilde{\beta}}{\sqrt{(\tilde{\alpha}_1)}} \cos\frac{\phi}{2} \quad (36)$$

$$= 1.73 \cos\frac{\phi}{2} \text{ for } \theta = g_1 \quad (37a)$$

$$= 1.64 \cos\frac{\phi}{2} \text{ for } \theta = g_4. \quad (37b)$$

The exact solution to this problem can be found in Grosh and Cess [22] who transformed the equation to a standard form of one-dimensional heat equation. The heat-transfer result is:

$$\frac{N_D}{\sqrt{(R_D Pr)}} = 1.60 \cos\frac{\phi}{2}. \quad (38)$$

The present method is again shown to yield satisfactory results.

5. CONCLUDING REMARKS

The primary purpose of this paper is to present a simple procedure for practical calculations of heat transfer in boundary layers. Oversimplified and, in fact,

improper profiles are deliberately used in the calculations, and the principal merit of the method, namely, the remarkable combination of simplicity and accuracy, is amply demonstrated and fully exploited. No effort is expended here in providing the details of the flow field.

Results of these calculations indicate that the rudimentary application of the method, as described in this paper, is adequate for most engineering purposes. The weak dependence of the results to the profiles continues to prevail. This is believed to be a consequence of using an integral expression for the surface heat flux; the effect of improper profiles is mostly reflected in the somewhat spurious predictions of transverse scales of the boundary layers, δ and δ_T, so that the predictions of the wall heat-flux remain reasonably accurate. However, near the thermal boundary-layer blow-off where the heat-transfer rates are small, the results are useful only for qualitative purposes. This finding is reminiscent of the difficulty encountered in the previous skin-friction calculations [1, 2].

The possibility of using the method to study general problems of transient heat conduction appears promising and warrants further investigation.

REFERENCES

1. T. F. Zien, A new integral calculation of skin friction on a porous plate, *AIAA Jl* **9**, 1423–1425 (1971).
2. T. F. Zien, Skin friction on porous surfaces calculated by a simple integral method, *AIAA Jl* **10**, 1267–1268 (1972).
3. V. N. Volkov, A refinement of the Karman Pohlhausen integral method in boundary-layer theory, *Inzh. Fiz. Zh.* **9**, 583–588 (1965). (English translation in *J. Engng Phys.* **9**, 371–374.)
4. L. G. Whitehead, An integral relationship for boundary layer flow, *Aircraft Engng* **21**, 14–16 (1949).
5. T. F. Zien, An approximate calculation of heat transfer in transpired boundary layers, NOLTR 73–17, Naval Ordnance Laboratory, White Oak, Md. (Feb. 1973).
6. K. Gersten and H. Körner, Wärmeübergang unter Berücksichtigung der Reibungswärme bei laminaren Keilströmunger mit veränderlicher Temperatur und Normalgeschwindigkeit entlang der Wand, *Int. J. Heat Mass Transfer* **11**, 655–673 (1968).
7. A. Fage and V. M. Falkner, Relation between heat transfer and surface friction for laminar flow, ARC RM 1408 (1931).
8. M. J. Lighthill, Contributions to the theory of heat transfer through a laminar boundary layer, *Proc. R. Soc.* **202A** 359–377 (1950).
9. G. W. Morgan and W. H. Warner, Heat transfer in laminar boundary layers at high Prandtl number, *J. Aeronaut. Sci.* **23**, 937–948 (1956).
10. N. Curle, *The Laminar Boundary Layer Equations*, Chapter 6. Clarendon Press, Oxford (1962).
11. B. T. Chao, An improved Lighthill's analysis of heat transfer through boundary layers, *Int. J. Heat Mass Transfer* **15**, 907–920 (1972).
12. H. Schlichting, *Boundary Layer Theory*, 6th edn, Chapter 12. McGraw-Hill, New York (1968).
13. W. E. Stewart and R. Prober, Heat transfer and diffusion in wedge flows with rapid mass transfer, *Int. J. Heat Mass Transfer* **5**, 1149–1163 (1962).
14. E. R. Thompson, High Prandtl number boundary layers with mass injection, *AIAA Jl* **7**, 547–548 (1969).
15. H. W. Emmons and D. C. Leigh, Tabulation of the Blasius function with blowing and suction. ARC TR 15966, C.P. No. 157 (1964).
16. R. Narasimha and S. S. Vasantha, Laminar boundary layer on a flat plate at high Prandtl number, *Z. Angew. Math. Phys.* **17**, 585–592 (1966).
17. D. R. Kassoy, Injection effects in high Prandtl number boundary-layer flows, *AIAA Jl* **6**, 1796–1797 (1968).
18. K. Gersten, Wärme- und Stoffübertragung bei großen Prandtl-bzw. Schmidtzahlen. *Wärme- und Stoffübertragung* **7**, 65–70 (1974).
19. V. N. Volkov and V. K. Li-Orlov, A refinement of the integral method in solving the heat conduction equation, *Heat Transfer-Soviet Res.* **2**, 41–47 (1970).
20. T. R. Goodman, Application of integral methods to transient nonlinear heat transfer, *Adv. Heat Transfer* **1**, 55–122 (1964).
21. H. S. Carslaw and J. C. Jaeger, *Conduction of Heat in Solids*, 2nd edn, Chapter 15, p. 388. Oxford University Press, Oxford (1959).
22. R. J. Grosh and R. D. Cess, Heat transfer to fluids with low Prandtl numbers for flow across plates and cylinders of various cross section, *Trans. Am. Soc. Mech. Engrs* **80**, 667–676 (1958).

ETUDE APPROCHEE DU TRANSFERT DE CHALEUR DANS LES COUCHES LIMITES DE TRANSPIRATION AVEC EFFET DU NOMBRE DE PRANDTL

Résumé—On a développé une procédure simple qui permet des calculs approchés des taux de transfert thermique pariétal dans les couches limites de transpiration. Les applications de cette procédure sont illustrées par des exemples variés d'écoulements laminaires incompressibles, pour des nombres de Prandtl faibles et élevés. Une limite remarquable aux grands nombres de Prandtl avec un faible taux de transfert massique est aisément identifiée, et quelques solutions limites sont présentées pour la configuration d'une plaque poreuse. Les calculs, effectués dans les cas avec faibles nombres de Prandtl, montrent clairement l'utilité de la méthode dans l'étude des problèmes transitoires de conduction thermique. La remarquable association de la précision à la simplicité constitue la qualité essentielle de la méthode.

ANGENÄHERTE ANALYSE DES WÄRMEÜBERGANGS IN DURCHLÄSSIGEN GRENZSCHICHTEN MIT EFFEKTEN DER PRANDTL-ZAHL

Zusammenfassung—Für Näherungsrechnungen des Wärmeübergangs an der Wand bei durchlässigen Grenzschichten wird ein einfaches Verfahren angegeben. Anwendungen dieses Verfahrens werden für verschiedene Beispiele gezeigt für inkompressible laminare Strömungen bei großen und kleinen Prandtl-Zahlen. Eine deutliche Grenze für große Prandtl-Zahl und kleine Stoffübergangsrate wird aufgezeigt

und einige Grenzlösungen werden für den Fall der porösen Platte wiedergegeben. Berechnungen mit kleinen Prandtl–Zahlen zeigen deutlich die Nützlichkeit der Methode bei der Untersuchung instationärer Wärmeleitprobleme. Die bemerkenswerte Kombination von Genauigkeit und Einfachheit stellen den Hauptvorteil der Methode dar.

ПРИБЛИЖЕННЫЙ АНАЛИЗ ПЕРЕНОСА ТЕПЛА В ПОГРАНИЧНОМ СЛОЕ В ПРОЦЕССЕ ПОРИСТОГО ОХЛАЖДЕНИЯ ПРИ ВЛИЯНИИ ЧИСЛА ПРАНДТЛЯ

Аннотация — Разработана простая методика приближенного расчета скорости переноса тепла в пограничном слое на стенке при пористом охлаждении. Применение методики иллюстрируется на различных примерах несжимаемого ламинарного течения жидкости для больших и малых значений числа Прандтля. С ё помощью легко определяется предел больших значений числа Прандтля и небольших значений скорости переноса массы. Представлены некоторые предельные решения для пористой пластины. Расчеты для случаев малых значений числа Прандтля явно свидетельствуют о пригодности метода для изучения проблемы нестационарной теплопроводности. Удивительное сочетание точности и простоты является основным достоинством метода.